Published in the International Journal for Engineering Structures, Vol. 26, Issue 3, February 2004, pp. 391-402.

Influence of Soil–Foundation–Structure Interaction on Seismic Response of the I-880 Viaduct

Boris Jeremić [1] **Sashi Kunnath** [2] **Feng Xiong** [3]

Abstract

The role of Soil–Foundation–Structure (SFS) interaction on seismic behavior of an elevated highway bridge (the I-880 viaduct) with deep foundations is investigated in this paper. A series of time domain, inelastic finite element simulations of seismic behavior of a bridge bent subjected to various earthquake events is carried out using two separate models of the system. The first model assumes the bridge columns to be rigidly connected to the foundation without SFS interaction. The second model incorporates SFS interaction through the use of equivalent springs. The spring properties are derived from three-dimensional finite element analysis of the pile foundation in a layered soil system. The analysis is based on nonlinear inelastic characteristics of the concrete substructure and linear elastic behavior of the soil-foundation system which was determined to be a reasonable assumption for this case study. The ground motions used in the simulation studies describe the expected hazard at the site and represent earthquakes with a 10% probability of being exceeded in 50 years. Results of the analysis indicates that SFS interaction can have both beneficial and detrimental effects on structural behavior and is dependent on the characteristics of the earthquake motion.

Keywords: Seismic soil–structure interaction.

[1] Department of Civil and Environmental Engineering, University of California, One Shields Ave., Davis, CA 95616, Email: `Jeremic@ucdavis.edu`.

[1] Department of Civil and Environmental Engineering, University of California, One Shields Ave., Davis, CA 95616,

[1] Sichuan University, Chengdu, China 610065, and formerly Visiting Researcher, University of California at Davis

1 Introduction

It is widely believed that the soil–foundation–structure (SFS) interaction is beneficial to the behavior of the structural system under earthquake loading. The Applied Technology Council's development of seismic regulations (known as ATC-3) propose simple formulae for computing fundamental period ($\tilde{T}$) and the effective dumping ratio ($\tilde{\beta}$) of structures founded on mat foundations on a homogeneous half-space. All codes today use an idealized envelope response spectra which attain constant acceleration values up to certain period (of order of 0.4 second to 1.0 second at most) and then *decrease monotonically with period* (for example as $T^{-2/3}$). As a consequence, SFS interaction leads to smaller accelerations and stresses in the structure and thereby smaller forces onto the foundation. The beneficial role of SFS interaction has been essentially turned into dogma for many structural engineers. Even the NEHRP-94 seismic code states that: *"These [seismic] forces therefore can be evaluated conservatively without the adjustments recommended in Sec. 2.5 [i.e. for SFS interaction effects]"*. Eventhough design spectra are derived on a conservative basis, and the above statement may hold for large class of structures, there are case histories that show that the perceived role of SFS interaction is an over–simplification and may lead to unsafe design.

Recent case studies suggest that the soil–structure interaction can be detrimental (e.g. Gazetas and Mylonakis [7]). In this paper it is demonstrated that, depending on the characteristics of the earthquake loading, the SFS interaction can be detrimental to the behavior of structure.

A number of papers in recent years have investigated the influence of the SSI on behavior of bridges [9,11,10,23,16,4,6]. In particular Sweet [23] and McCallen and Romstadt [16] performed a finite element analysis of bridge structures subjected to earthquake loads. However, Sweet [23] did approximate the geometry of pile groups as he was unable to analyze a full model with available computer hardware. On the other hand, McCallen and Romstadt [16] performed a remarkable full scale analysis of the soil–foundation–bridge system. The soil material (cohesionless soil, sand) was modeled using equivalent elastic approach (using Ramberg–Osgood material model through standard modulus reduction and damping curves developed by Seed et al. [19]). The two studies by Chen and Penzien [4] and by Dendrou et al. [6] analyzed the bridge system including the soil but the developed models used a very coarse finite element meshes.

The present study is part of a ongoing effort to document the importance of including soil-structure interaction effects in seismic response analysis of bridge structures. Most of the elevated highway structures in California rest on pile foundations with varying soil profiles. Preliminary analytical studies comparing the response of fixed-base models with simplified soil-foundation models are expected to provide important information on the need for considering soil-structure interaction effects in the design process. The testbed structure considered in the present evaluation is a typical bent from an actual highway bridge structure, the I-880 viaduct in Oakland, California. This recent structure is a replacement for the Cypress Freeway structure that failed during Loma Prieta Earthquake in 1989.

2 The Simulation Model

A simulation model of the highway structure is being developed systematically in increasing level of detail and complexity. This paper focuses on a model of a typical bent of the I880 highway structure in Oakland, CA. The simulation model was developed for use in the computer platform OpenSees [18]. The model is composed of inelastic fiber beams to represent the bridge piers where much of the inelastic behavior is expected to occur, elastic beams to represent the deck and equivalent zero-length foundation springs to represent the entire soil-foundation system. Foundation springs were obtained from a detailed 3D finite element model of the pile group foundation system using elastic soil properties. The soil-foundation modeling is described in Section 2.2. The nonlinear fiber beam element is prismatic with each integration point being identified by a section description. Each section is discretized into fibers composed of rebars, cover concrete and core concrete. Inelastic uniaxial stress-strain behavior is prescribed for each material type used to discretize the section. The integration along the element is based on Gauss-Lobatto quadrature rule. In the present formulation, four integration points are used with two integration points at the element ends. An iterative form of the flexibility formulation is used which is expected to improve the rate of global convergence at the expense of more local element computation. Additional details on the nonlinear beam element can be found in the User Manual documentation for OpenSees (Mazzoni et al. [15]).

2.1 Description of Structure

The selected system is a seven-frame structure consisting of 26 spans and a total length of approximately 1140 m. The site is located within 10 km of the Hayward Fault and is also in the immediate vicinity of the San Andreas Fault. In addition, the soils on the site near the San Francisco Bay consist of dense fill, Bay mud and sand, covering deep clay deposits. The superstructure of the viaduct is composed of 7 cast-in place reinforced concrete box girders, approximately 21.8 m wide, 2.0 m tall and 0.3 m in depth. In general, the bents have two columns. However, some of the bents have three or four columns at the location of the off-ramp while some of the remaining bents have outriggers. Most of the piles are 60 cm diameter with nominal 3560 kN capacity. The 55 columns for the viaduct are rectangular with circular reinforcement. While a majority of the columns have continuous moment connections at the column-deck and column-pile-cap region, some bents have pinned connections at either the column-pile-cap or column-deck location. Transverse reinforcement consists of #8 (2.5 cm diameter) hoops at 10 cm center-to-center spacing for all columns. Longitudinal reinforcement consists of varying numbers of #14 (4.5 cm) bars arranged in 5 different configurations. A typical bent was first selected for detailed evaluation. This bent (identified in the design drawings as Bent 16) has a cross section of 260 cm by 245 cm. The longitudinal reinforcement in the columns consists of 36-#14 bars. The columns in this bent have fixed connections at both the top and base which is typical in 24 of the 55 columns of the viaduct. The bent configuration and section details are shown in Figure 1.

The selected bent was modeled using nonlinear fiber-beam models for the columns and elastic beam models for the deck. Since the deck is composed of heavy box girders with longitudinal and transverse prestressing, it was assumed that the girder section of the bent could be modeled as an elastic element.

The following sections describe the modeling of material behavior, and are based on design specifications listed in the structural drawings.

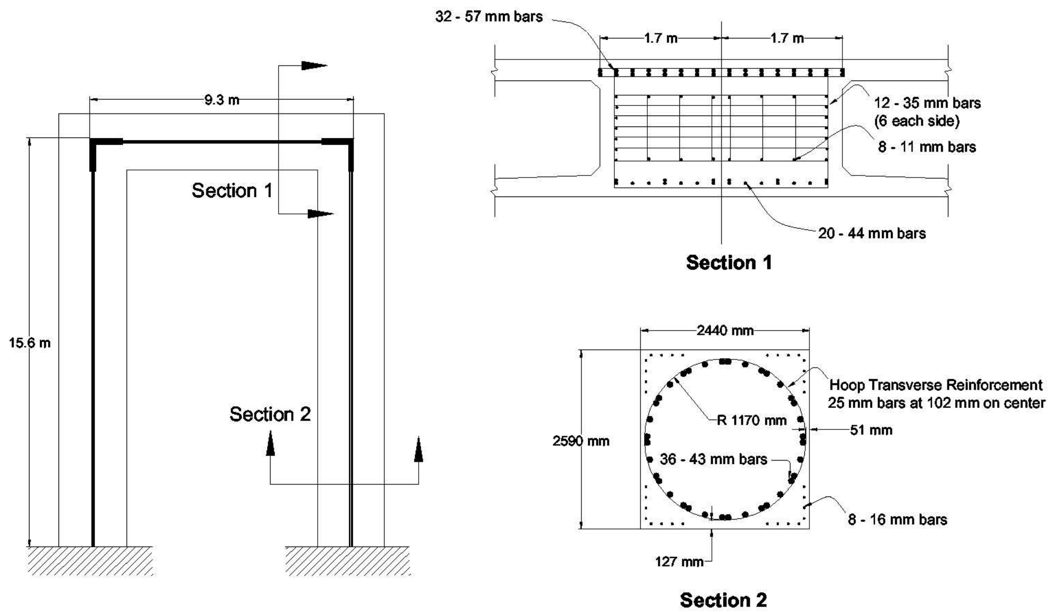

Fig. 1. **Bent configuration and section details.**

2.1.0.1 Concrete Modeling. There are numerous uncertainties associated with modeling the nonlinear behavior of concrete. Consequently, a simple concrete material model with no tensile strength was adopted. The behavior in compression is modeled as:

$$f_c = f'_c \left[\frac{2\epsilon}{\epsilon_0} - \left(\frac{\epsilon}{\epsilon_0} \right)^2 \right] \qquad \text{when} \qquad \epsilon \leq \epsilon_0 \tag{1}$$

where f_c is the stress, ϵ is the corresponding strain, f'_c is the compressive strength of the concrete and ϵ_0 is the strain at peak strength. The above expression is valid up to peak strength. Softening beyond the maximum compressive strength is approximated as a linear function. A residual strength may also be specified at ultimate strain. The material properties selected for the modeling of the bent is shown in Figure 2. The confined strength of concrete was estimated using the Mander model (Mander et al. [12]). A residual strength of 16 MPa was assigned to the confined core while no residual strength was assigned to the cover concrete.

2.1.0.2 Modeling of Steel Reinforcement. A bilinear model with strain hardening was specified for the main reinforcing steel. The expected cyclic behavior of the steel is shown in Figure 3. The yield strength of the steel was

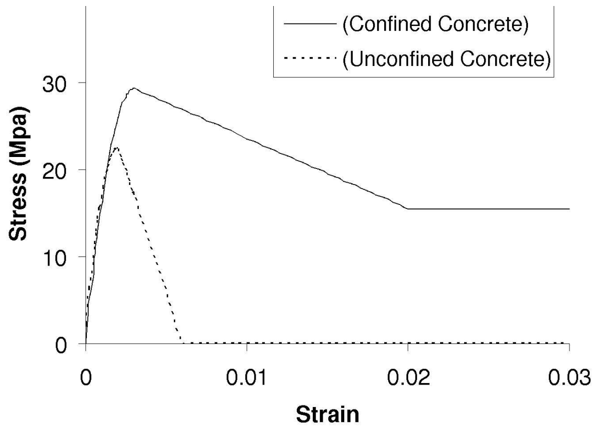

Fig. 2. **Stress–Strain modeling of concrete.**

specified as 455 MPa. A 1% post-yield stiffness is used to describe the hardening of steel beyond yield.

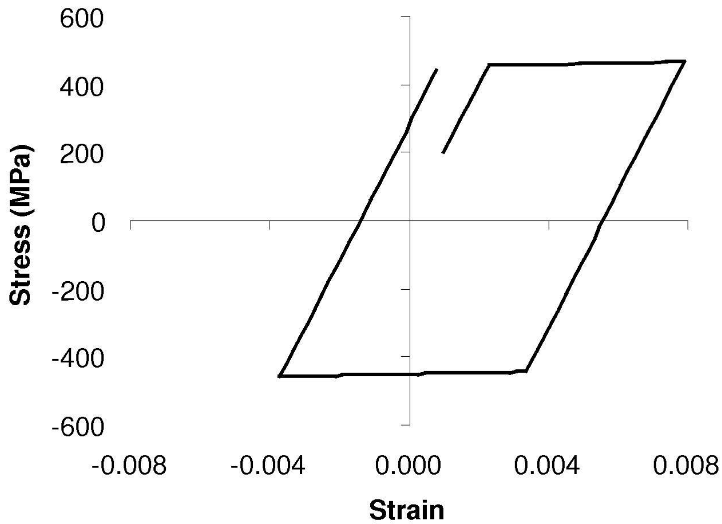

Fig. 3. **Assumed Stress–Strain behavior of reinforcing steel.**

A sensitivity analysis was carried out to determine the level of the core discretization required to obtain reliable results. Several discretizations were evaluated and the final model selected for ensuing analysis is shown as Model C in Figure 4.

2.2 Foundation System and Soil

The foundation system consists of a 5×5 pile groups connected with a massive pile cap. The piles are made of reinforced concrete and reside in a steel shell

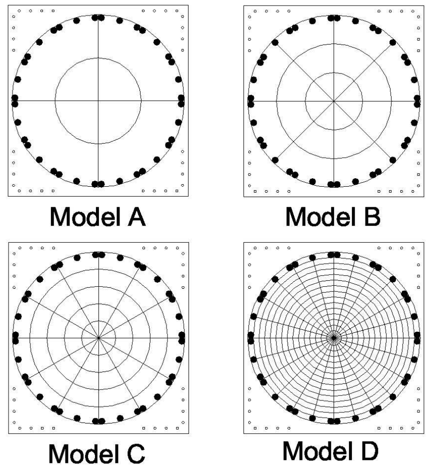

Fig. 4. **Alternative discretizations for the cross section; Model C was selected for analysis.**

with a diameter of 0.6m. The schematic figure of the pile cap and the piles is show in Figure 5.

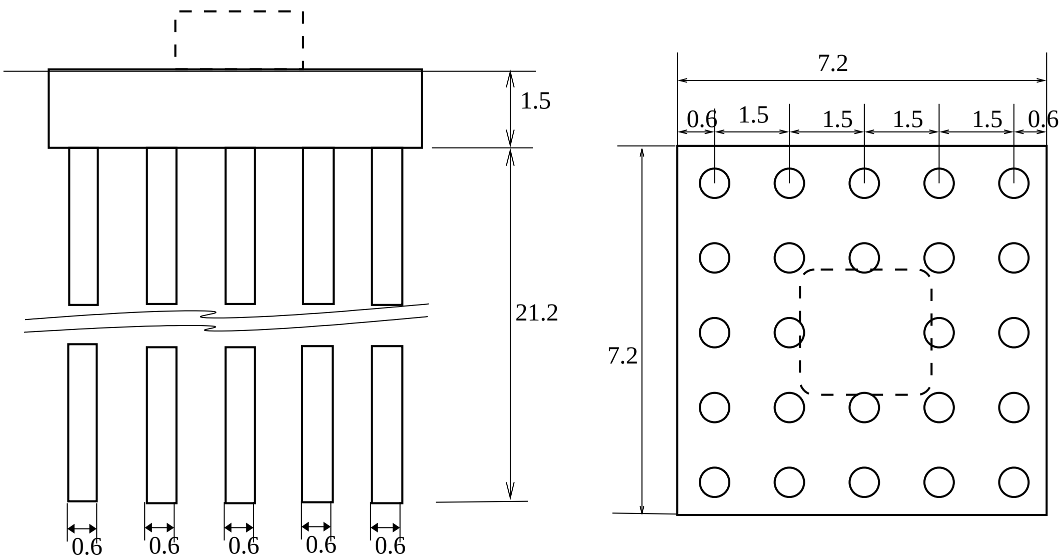

Fig. 5. **Schematics of the pile cap and the piles.**

The soil surrounding the pile groups for this bent can be divided in three layers. The top layer of 3m is made up of dense fill sand, middle 9m layer is soft Bay Mud while the lower soil layers are composed of alluvial sand. While the soils surrounding the foundation system are inelastic, an elastic representation has been utilized in this study. This simplification to elastic soil is done for two primary reasons: (1) for the fully saturated clay surrounding the piles, the expected deformations are expected to be very small; and (2) to save computational time associated with a full 3D inelastic iterative dynamic analysis of the subsurface,foundation system and the structure. Clearly, nonlinearity in the soil material can arise purely due to wave propagation. However, recent work on the behavior of pile groups by Yang and Jeremic ([24]) has shown that for relatively small displacements, the initial behavior of large pile groups (such as the one considered in this study) is elastic.

In fact, since the soft clay material is fully saturated, and the loading is very rapid (earthquake load lasting less than a minute) the pore water dissipation is negligible thus resulting in almost full elastic response, with solid "soil skeleton" not having time to respond to loads, and pore water behaving as "elastic pillows". The only resistance of the solid skeleton of soil that will have an effect is in shear and in this case, there is not enough movement of the pile head and on the top portion of piles to activate fully shear resistance. Additionally, liquefaction potential at this site is very small.

Based on these facts, it was determined that an elastic soil model would be an adequate approximation for this case study. The elastic properties for the dense fill sand were chosen as $E = 20,000.00kPa, \nu = 0.3$, the alluvial sand in deep layers $E = 17,400.00kPa, \nu = 0.3$ (based on work by [13]), and for the soft Bay Mud $E = 12,000.00kPa, \nu = 0.3$ (based on data by[3]). The assumption of an elastic soil is expected to influence the results by reducing the amount of inelastic energy dissipation in the foundation system. It must be reiterated that this assumption is valid only for the case study presented here and should not be construed as a generally valid approach for all cases. Additional work is ongoing using a fully elastic–plastic model of this foundation system, including the effects of potential horizontal spreading from nearby sand deposits.

The foundation system model was developed in a hierarchical fashion beginning with two simple models. The simplest foundation model consisted of a fully fixed support in all directions. The second foundation model comprised linear translational and rotational springs. The effects of soil nonlinearities were neglected for this particular type of clay for reasons cited previously. One feature that is missing is radiation damping which is clearly an important issue that can influence foundation-soil-structure interaction. Since radiation damping is a result of the stiffness differences between the piles (including pile cap) and the surrounding soil, it manifests primarily at higher frequencies and low soil damping. If gaps open between the foundation and soil, there can be no radiation damping. Hence, the accurate modeling of radiation damping, particularly if the top soil layers are cohesive, can be complex. A simple approach that has been adopted by many researchers (e.g. Maragakis and Jennings [14] Spyrakos [22], Zhang and Makris [26]) is to use frequency independent springs and dashpots to represent the soil-foundation system. Such models, however, do not consider possible gaps during seismic excitation. Given the uncertainties in modeling the overall soil-foundation behavior and the fact that frequency independent dashpots generally deamplify the structural system response, it is not uncommon to neglect radiation damping altogether. In their investigation of the observed behavior of a two-span overcrossing, Makris et al. [11] are able to simulate the response of the bridge without the need for radiation damping. The simulations by Ciampoli and Pinto [5] also do not incorporate radiation damping. Additionally, recent investigations by Bielak et al. (cf. [2,25]) indicate that in some cases radiation damping can be ignored with minor effects on the system behavior. Thus, based on data from previous studies and the fact that the bridge pier yields well before the soil deformations become significant, the effects of radiation damping are not considered.

The spring constants for the simplified foundation system were obtained from an analysis of a full 3D foundation model, using linear elastic material properties for both the soil and the concrete piles. Figure 6 shows the finite element mesh for this model. The model is made of solid 20 node quadratic brick elements for the soil and pile group cap, while elastic (Bernoulli) beam elements are used for piles. The model has approximately 1300 solid finite elements, 127 linear beam elements. The total number of unknowns is close to 2000. The boundary conditions were set to full support at the bottom of the model, and the sliding face at the four vertical faces of the model. Loading was separated in two stages, first stage was the self weight, while the second stage was a static pushover at the top of the column. The elastic material model used for soil material were as follows (): Young's modulus $E = 11000kPa$, Poisson's ratio $\nu = 0.45$ and unit weight of clay was set to $\gamma = 13.7kN/m^3$. This mixing of solid and structural element exhibits two potential problems. The displacement interpolation function for beam elements (l'Hermite polynomials) and solid elements (quadratic polynomials) are incompatible. This might result in interpenetration (numerically) of pile material into soil material. In addition to that, the solid soil elements occupy volume that would be taken by

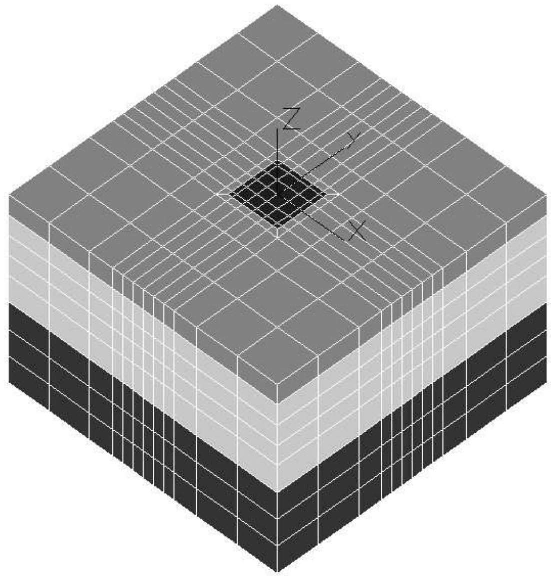

Fig. 6. **Finite element mesh for the pile group foundation and soil.**

the beam element (concrete pile). However, the model is simple enough and when linked to elastic assumption for soil, provides a good balance between sophistication and simplicity.

3 Seismic Simulation Results

3.1 Static Pushover Analysis

A static pushover analysis was conducted for two different bent models. The difference between these models was in the treatment of the foundations. Model # 1 had a fixed foundation (no soil structure interaction) while the model # 2 did include soil structure interaction effects in the form of soil springs. Soil springs were obtained by analyzing a full 3D model for the soil and foundation substructure (described in section 2.2). Figure 7 shows two types of foundation treatment for Bent #16.

The stiffness of the springs, obtained from the elastic analysis of the full 3D model of the pile group and the soil are given in table 1.

The load displacement response of the Bent # 16 is shown in Figure 8(a).

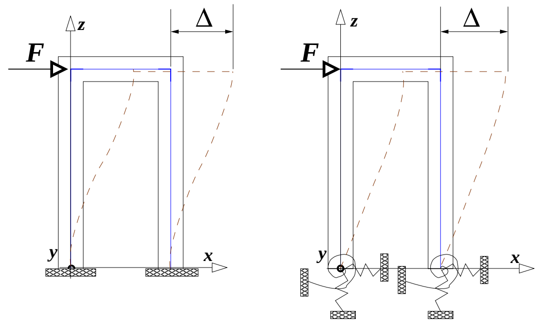

Fig. 7. **Two frame models for the Bent #16,fully fixed and the model with soil springs.**

Degree of Freedom	Spring Stiffness
Axial (vertical, z direction)	$5.018e^5\ kN/m$
Transversal (horizontal, x and y directions)	$1.138e^5\ kN/m$
Torsional (around vertical, z axes	$6.447e^6\ kNm$
rocking (around horizontal, x and y axes)	$7.813e^6\ kNm$

Table 1

Spring stiffness for elastic foundation system.

In order to establish the natural period values for generation of earthquake spectra, after each stage of static pushover, an eigenvalue analysis was performed. In particular, three horizontal loading levels were targeted. The first loading level was at no horizontal load, with only the self weight acting on the bent. The second loading level was set after the initial cracking has occurred. In this particular case, this load level is similar for both models, as the soft foundation will affect the displacements but not the load level for static pushover. This load level was set at approximately $4,500$ kN. The third load level was set close to the limit point for both cases (again, very similar load capacity, but different displacements). This load level was set at approximately $10,200$ kN. These three load levels were given notations based on the state of the structural model: elastic, cracked and yielded. The variations of the fundamental period with increasing inelasticity of the system results are summarized in Figure 8(b). It is evident that for the case where the base is assumed to be fixed, the pier response becomes nonlinear very early in the response with yielding taking place at a lateral deck displacement of approximately 0.1 m. However, for the case when equivalent soil-foundation springs are included, the response is essentially elastic till 0.4m of lateral displace-

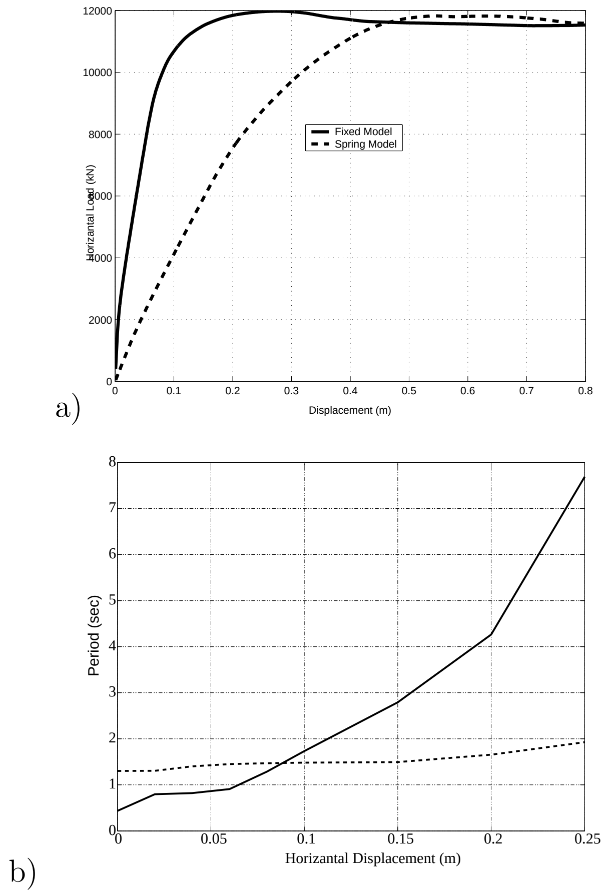

Fig. 8. **Fully supported and elastic springs results for Bent # 16 shown: (a) Load – displacement response for static pushover analysis, (b) Period – displacement response from eigenvalue analysis for different stages of static pushover tests.**

ment. The additional flexibility introduced by the soil-foundation system will play an important role in altering the overall response of the bridge system depending on the characteristics of the ground motion, as will be demonstrated later in this paper.

3.2 Ground Motions

A uniform hazard spectra for SD (soil) site conditions was derived for a site in Oakland which represents an event with a 10 % probability of exceedance in 50 years. The hazard is dominated by earthquakes on the Hayward fault which is located about 7 km east of the I–880 site. The ground motion model of Abrahamson and Silva [1] was used in generating the spectra (Somerville and

Collins [20]). The spectra contains rupture directivity effects which were represented in the probabilistic hazard analysis using the empirical model proposed by Somerville et al. [21]. The spectra were generated for both fault-parallel (FP) and fault-normal (FN) directions. Several earthquake records with the required magnitude-distance combinations from strike-slip earthquakes were considered. Details of the process of generating the final ground motions are described in Somerville and Collins [20].

For the purpose of this study, three time histories were selected: two from the modified suite of Loma Prieta motions (recorded at Gilroy and Corralitos) and one from Kobe. The components in the fault normal (FN) directions of each of these records needed to be scaled to match selected period points on the hazard spectra. The period values selected correspond to the previously mentioned states of the structural model: elastic, cracked and yielded. The period values were established through eigenvalue analysis of the fixed-base model and the foundation-spring model at different load–displacement levels during the pushover analysis. The particular load and displacement levels were discussed in section 3.1.

The period values selected for scaling of the records are shown in Table 2. Comparison of the spectra of the selected time histories with the Hazard Spectra provided the scale factors to be used. These are also listed in Table 2 for both structural models at all three states of the system. The same scale factor is used for both FP and FN histories since it preserves the relative scaling between all components of the recording.

Finally, in order to use the time-histories, it was necessary to determine the alignment of the bent to the FN and FP directions of the fault. It was established that Bent 16 was inclined to the FP direction by 20 degrees (see figure 9 obtained from a satellite photo [8]). The following relationship was then used to transform the scaled time histories.

$$TransverseComponent = FP\cos\theta + FN\sin\theta \tag{2}$$

The response spectra of the resulting time-histories are displayed in Figures 10(a)-(f).

[1] corresponds to the spectral acceleration (Sp. Ac) at the designated period value.

Table 2

Scaling of Earthquake Records to Match Hazard Spectra.

		Hazard	LP–Gilroy		LP–Corralitos		Kobe	
Tag	Period	**Spectra**	Sp. Ac [1]	**Scale**	Sp. Ac [1]	**Scale**	Sp. Ac [1]	**Scale**
Fixed–Based Model								
A	0.37	**1.470**	0.611	**2.41**	1.146	**1.28**	2.482	**0.59**
B	0.77	**1.053**	0.268	**3.94**	1.349	**0.78**	2.482	**0.42**
C	1.54	**0.699**	0.311	**2.25**	0.239	**2.92**	0.709	**0.99**
Spring–Based Model								
D	1.24	**0.820**	0.301	**2.72**	0.376	**2.18**	0.922	**0.89**
E	1.60	**0.675**	0.285	**2.37**	0.193	**3.50**	0.639	**1.06**
F	2.00	**0.513**	0.170	**3.02**	0.175	**2.93**	0.422	**1.22**

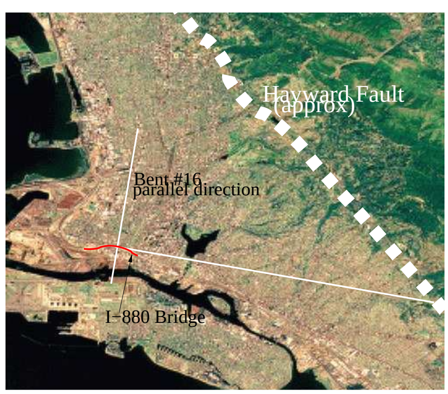

Fig. 9. **Position of the I-880 Bridge and the Bent # 16 with respect to the location of Hayward Fault (from satellite photo).**

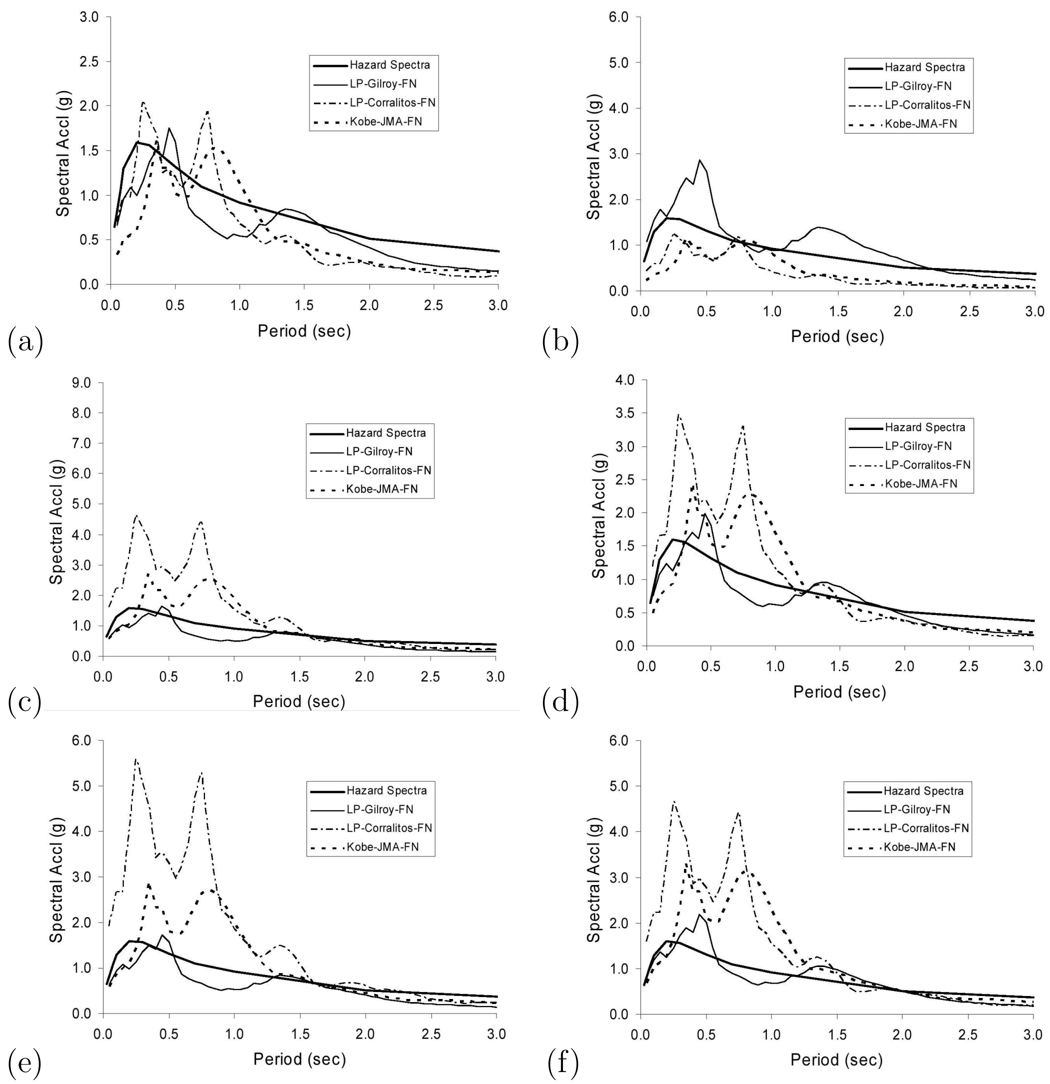

Fig. 10. **Response Spectra of Scaled Accelerograms. Fixed-Base Model Matched Hazard Curve at (a) T = 0.374 sec ; (b) T = 0.77 sec; (c) T = 1.54 sec ; Soil-Spring Model: Matched Hazard Curve at (d) T = 1.2 sec ; (e) T = 1.6 sec ; (f) T = 2.0 sec .**

3.3 Seismic Analysis

In this section, representative results for both fixed and spring supported models of Bent subjected to scaled earthquake excitations are presented. The main feature in evaluation of the two bent models is in different behavior of the same bent for given input motions. Namely, the response of structure to some earthquake motions will benefit from SSI, in other cases SSI will be detrimental to the behavior of structure and in some cases the effects will not be significant.

The effects of SFS interaction are considered to be beneficial to the structure under the following conditions:

- There are no significant permanent deformations in the structure resulting from yielding of the pier, or
- The energy dissipation (hysteretic loops) of the system with SSI is smaller than that with fixed foundation, leading to the conclusion that there is less damage to the structure.

If any of the above criteria is not fulfilled, it is assumed that SSI is detrimental to the structure behavior. In some cases, the observations were inconclusive, hence these cases are reported as not being significant to the system response.

3.3.1 Beneficial Effects of SSI

The first set of results shows cases where the SSI was beneficial to the behavior of the structure. Figure 11 shows behavior of the bent subjected to the scaled Corralitos record (Tag B). This record was scaled to match the hazard spectra at a period of 0.77 sec. As is evident from the spectra shown in Figure 10, the demands imposed by the earthquake are more significant in the short period range, hence the fixed base model experiences higher demands than the model with soil springs. Both SSI and non–SSI results show small permanent deformation (on the order of one to two centimeters). However, the hysteretic loops of the model considering SSI effects are much smaller then those of the non–SSI model thus suggesting much smaller levels of damage for the SSI model.

Figure 12 shows results for both models subjected to the scaled Gilroy earth-

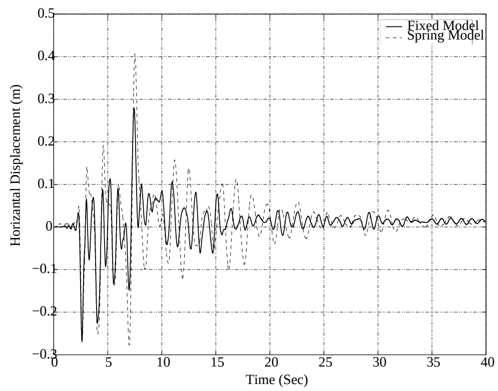

a)

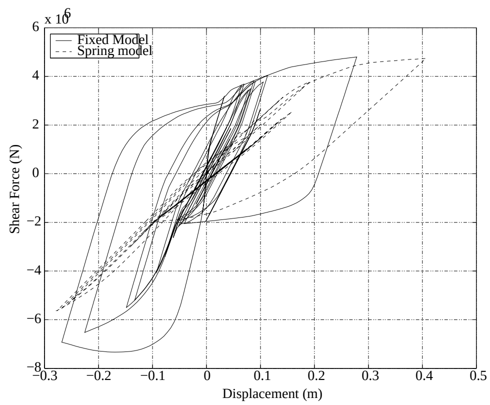

b)

Fig. 11. **LP–Corralitos (Tag B) Record : a) displacement time history for fixed and spring supported models, b) horizontal displacement vs shear force for fixed and spring supported models.**

quake (Tag B). Like the previous record, this was also scaled to a period of 0.77 sec. Though the spectral amplitudes show significant amplification in both the short and long period range, the demands in the short period are much higher than those in the long period region. Once the system becomes inelastic, the periods increase leading to even smaller demands for the flexible model (with soil-foundation springs) while the demands in the fixed model are still significant moving from the range between 0.4 - 0.6 seconds to the inelastic range between 1.2 - 2.0 seconds. Eventhough there are no permanent deformations in both SSI and non–SSI cases, the non–SSI case experiences much larger levels of damage, which is indicated by the size of hysteretic loops.

The SSI model (Figure 13) shows a primarily elastic response when subjected to the scaled Gilroy motion (Tag A). On the other hand, the non–SSI model experiences both permanent deformations and large energy dissipation, suggesting large levels of damage after the earthquake shaking. This Gilroy record was scaled to match the hazard spectra at 0.37 sec. Like the two previous

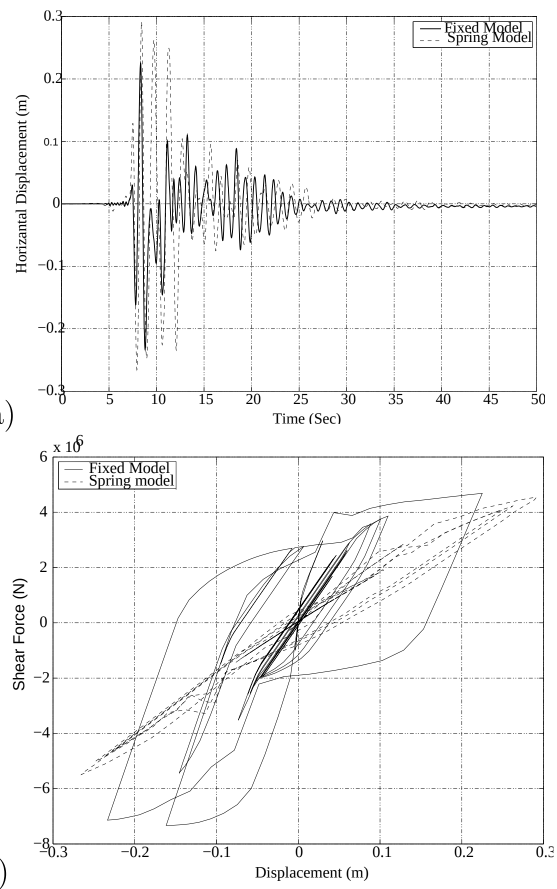

a)

b)

Fig. 12. **LP–Gilroy (Tag B) Record: a) displacement time history for fixed and spring supported models, b) horizontal displacement vs shear force for fixed and spring supported models.**

cases, the spectral accelerations are much higher for periods less than 1.0 sec which impacts the demands on the fixed base model more than the model with soil-foundation springs.

3.3.2 Detrimental Effects of SSI

This set of results show that in many cases SSI can be detrimental to the behavior of structure. For example, results in Figure 14, clearly indicate that the SSI model subjected to scaled Gilroy earthquake (Tag D) is dissipating more energy and also being subjected to larger deformations than the non–SSI model. The spectral demands are initially higher in the short period range for this record, however, it is likely that the fixed base model moves into a region of slightly lower demands (just beyond 0.5 seconds) since the degree of inelasticity is not severe. The shift in the period from 1.24 seconds of the soil-spring based model takes it into a region of increased demand thus causing

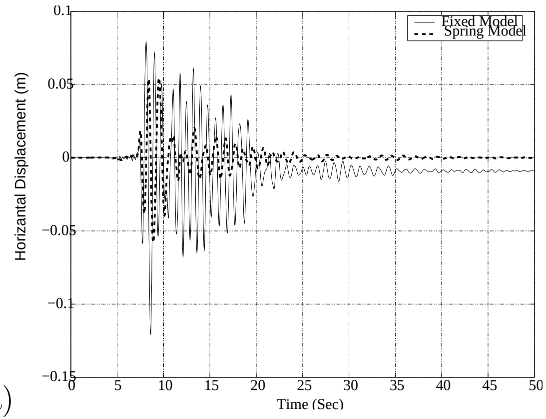

a)

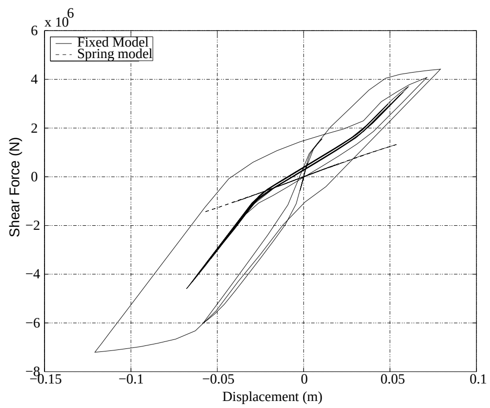

b)

Fig. 13. **LP–Gilroy (Tag A) Record: a) displacement time history for fixed and spring supported models, b) horizontal displacement vs shear force for fixed and spring supported models.**

higher drifts.

The effect of soil-structure interaction is much more pronounced when the models are subjected to the Corralitos record (Tag D). In this particular case, the size of the hysteretic loops (the amount of energy dissipated) is much larger for the SSI model. Once again, though the sharp peaks in the short periods seem to suggest the likelihood of higher demands for the fixed-base model, the demands actually drops from 0.37 seconds to 0.6 seconds. Hence it is clear that the dynamic response is extremely sensitive to shifts in the fundamental period as the structure moves from the elastic to the inelastic state. Such sensitivity makes it difficult to develop simplified guidelines for designing structures incorporating soil-structure interaction.

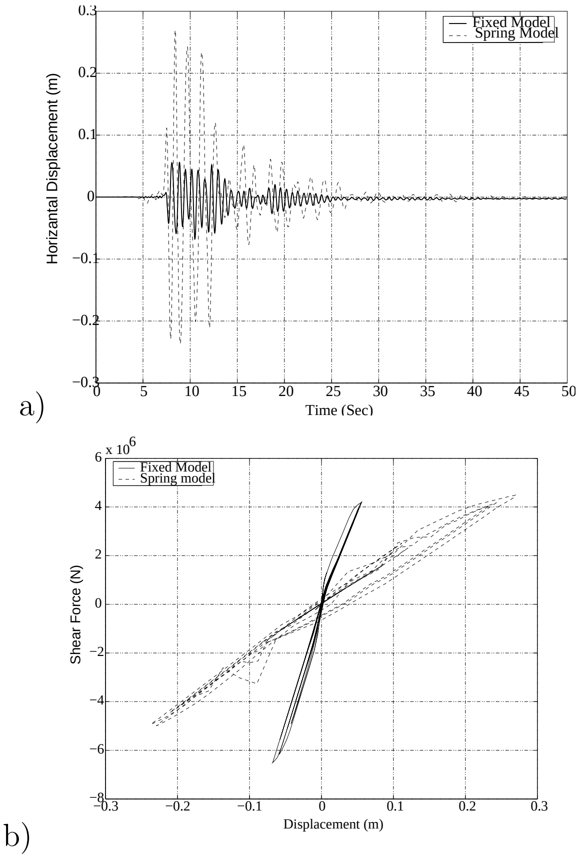

Fig. 14. **LP–Gilroy (Tag D) Record: a) displacement time history for fixed and spring supported models, b) horizontal displacement vs shear force for fixed and spring supported models.**

3.3.3 Effects of SSI Not Significant

This last sections shows results for which the effects of SSI are not clearly observable. For example Figure 16 shows results for a bent model subjected to scaled Corralitos earthquake (Tag F). Eventhough, there is apparently a small amount of permanent deformation for non–SSI model, the SSI model seems to have larger hysteretic loops, suggesting more damage to the structure. The displacements of the SSI model are higher, however, the displacements also include the rotation of the pile cap. The relative bent deformations are similar to those for the fixed-base model. In this particular case, both models show some evidence of inelastic behavior.

On the other hand, bent model subjected to the scaled Corralitos motion (Tag A), shown in Figure 17, presents similar behavior for both SSI and non–SSI models. Permanent deformation is observable in results for both models, and the amount of energy dissipation (size of hysteretic curves) is of comparable

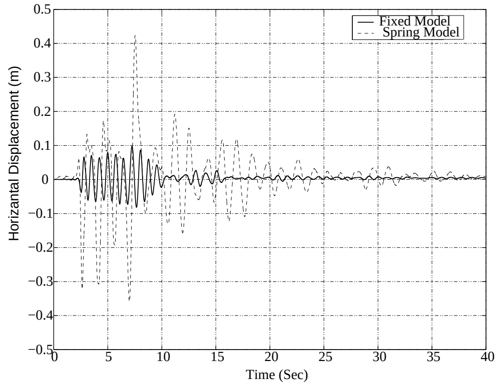

a)

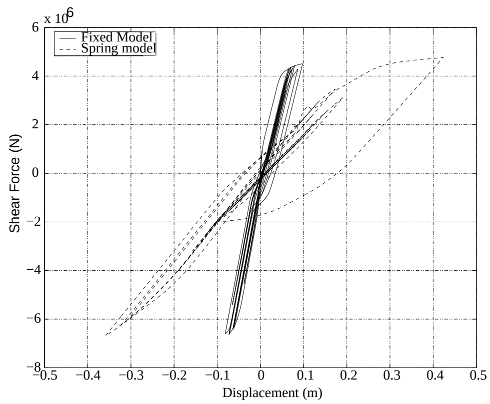

b)

Fig. 15. **LP–Corralitos (Tag D) Record: a) displacement time history for fixed and spring supported models, b) horizontal displacement vs shear force for fixed and spring supported models.**

magnitude as well. A general observation for all cases is that the SSI model results in higher drifts at the bent cap. As pointed out in the previous case, this is a consequence of the rotation of the pile cap. The relative tangential drift from the base of the pile cap to the top of the bent cap is similar in both models when SSI effects are not significant.

4 Future Directions

In this paper, the influence of soil–structure interaction (SSI) on a typical bent of an existing elevated highway bridge is evaluated.

A significant feature of the study is the systematic methodology employed to evaluate the system: beginning with the hazard description and leading up to the simulation model of a typical bent and the characterization of SSI effects.

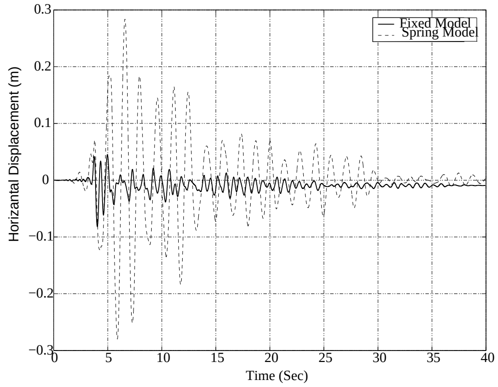

a)

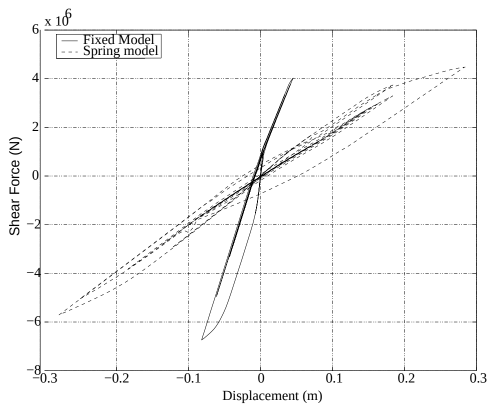

b)

Fig. 16. **LP–Corralitos (Tag F) Record: a) displacement time history for fixed and spring supported models, b) horizontal displacement vs shear force for fixed and spring supported models.**

It was shown that the SSI can have both beneficial and detrimental effects, and is dependent primarily on the characteristics of the ground motions. It is useful to mention that another recent study by Mylonakis and Gazetas ([17] support the conclusions reached in this paper that one of the Kobe earthquake components triggered more significant SSI effects than another Kobe component.

The plan for future work is to expand the structural model to include multiple bents in a single frame and eventually the consideration of multiple frames so that frame-to-frame interaction is considered. On the soil side, the plan is to analyze effects of soil inelasticity on SSI. Additionally, the seismic wave propagation along the length of the bridge will be investigated as well.

This investigation has also demonstrated the difficulty associated with developing guidelines for design since SSI effects are not only a function of the structural system and and the soil-foundation behavior but also dependent on

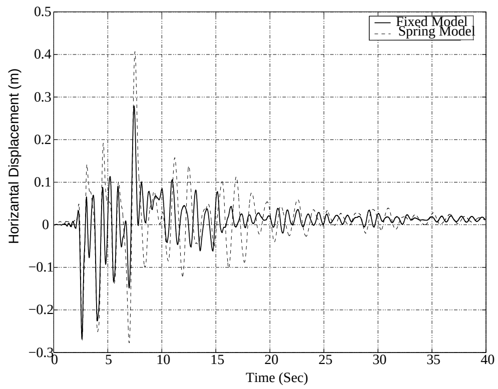

a)

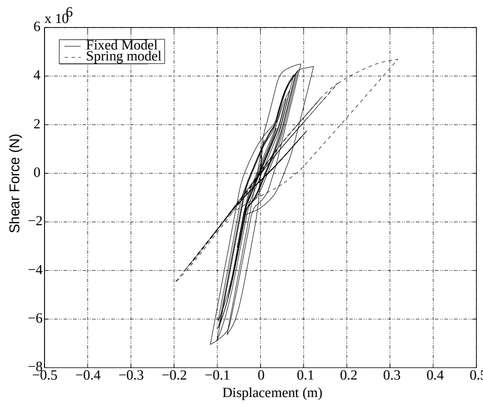

b)

Fig. 17. **LP–Corralitos (Tag A) Record: a) displacement time history for fixed and spring supported models, b) horizontal displacement vs shear force for fixed and spring supported models.**

the ground motion. In general, this suggests that SSI effects should be evaluated on a case-by-case basis without generalizing the findings of a particular study. However, the results documented here and those being reported in recent literature will provide a basis for developing guidelines for considering SSI effects in structural analysis of bridge structures.

Acknowledgment

This work is funded by a grant from the Pacific Earthquake Engineering Research (PEER) center which is supported in part by the Earthquake Engineering Research Centers Program of the National Science Foundation under Award Number EEC-9701568.

References

[1] N. A. Abrahamson and W. J. Silva. Empirical response spectral attenuation relations for shallow crustal earthqaueks. *Seismological Research Letters*, 68:94–127, 1997.

[2] Jacobo Bielak, Kostas Loukakis, Yoshaiki Hisada, and Chaiki Yoshimura. Domain reduction method for three–dimensional earthquake modeling in localized regions. part I: Theory. *Bulletin of the Seismological Society of America*, 93(2):817–824, 2003.

[3] Dan A. Brown and Chine-Feng Shie. Some numerical experiments with a three dimensional finite element model of a laterally loaded pile. *Computers and Geotechnics*, 12:149–162, 1991.

[4] M. A. Chen and J. Penzien. Nonlinear soil–structure interaction of skew highway bridge. Report UCB/EERC-77/24, Earthquake Engineering Research Center, 1977.

[5] M. Ciampoli and P.E. Pinto. Effects of soil-structure interaction on inelastic seismic response of bridge piers. *ASCE J. of Structural Engineering*, 121(5):806–814, 1995.

[6] B. Dendrou, S. D. Werner, and T. Toridis. Three dimensional response of a concrete bridge system to traveling seismic waves. *Computers and Structures*, 20:593–603, 1985.

[7] George Gazetas and George Mylonakis. Seismic soil–structure interaction: New evidence and emerging issues. In Panos Dakoulas, Mishac Yegian, and Robert D. Holtz, editors, *Proceedings of a Specialty Conference: Geotechnical Earthwuake Engineering and Soil Dynamics III*, Geotechnical Special Publication No. 75, pages 1119–1174. ASCE, August 1998. 1998.

[8] MapQuest Inc. `http://www.mapquest.com/`. Online version, 2002.

[9] A. J. Kappos, G. D. Manolis, and I. F. Moschonas. Sismic assessment and design of R/C bridges with irregular configuration, including SSI effects. *International Journal of Engineering Structures*, 24:1337–1348, 2002.

[10] N. Makris, D. Badoni, E. Delis, and G. Gazetas. Prediction of observed bridge response with soil–pile–structure interaction. *ASCE Journal of Structural Engineering*, 120(10):2992–3011, October 1994.

[11] N. Makris, D. Badoni, E. Delis, and G. Gazetas. Prediction of observed bridge response with soil-pile-structure interaction. *ASCE J. of Structural Engineering*, 120(10):2992–3011, 1995.

[12] J. B. Mander, M. J. N. Priestley, and R. Park. Theoretical stress-strain model for confined concrete. *ASCE Journal of Structural Engineering*, 114(8):1804–1826, 1988.

[13] M. T. Manzari and Y. F. Dafalias. A critical state two–surface plasticity model for sands. *Géotechnique*, 47(2):255–272, 1997.

[14] E. A. Maragakis and P.C. Jennings. Analytical models for the rigid body motions of skew bridges. *Earthquake Engineering and Structural Dynamics,*, 15(8):923–944, 1987.

[15] Silvia Mazzoni, Frank McKenna, Michael H. Scott, Gregory L. Fenves, and Boris Jeremić. *Open System for Earthquake Engineers Simulation (OpenSees) : User Manual.* Pacific Earthquake Engineering Research Center, Richmond, December 2002.

[16] D. B. McCallen and K. M. Romstadt. Analysis of a skewed short span, box girder overpass. *Earthquake Spectra*, 10(4):729–755, 1994.

[17] G. Mylonakis and G. Gazetas. Seismic soil-structure interaction: Beneficial or detrimental? *Journal of Earthquake Engineering*, 4(3):277–301, 2000.

[18] OpenSees Development Team (Open Source Project). OpenSees: open system for earthquake engineering simulations. `http://opensees.berkeley.edu/`, 1998-2003.

[19] H. B. Seed, R. T. Wong, I. M. Idriss, and K. Tokimatsu. Moduli and damping factros for dynamic analysis of cohesionless soils. Earthquake Engineering Research Center Report UCB/EERC 84/14, University of California Berkeley, 1984.

[20] Paul Somerville and Nancy Collins. Ground motions time histories for the I-880 bridge, Oakland. Report to peer methodology testbeds projects, URS Corporation, 2002.

[21] P.G. Somerville, N.F. Smith, R.W Graves, and N.A. Abrahamson. Modification of empirical strong ground motion attenuations to include the amplitude and duration effects of rupture directivity. *Seismological Research Letters*, 68:199–222, 1997.

[22] C. C. Spyrakos. Seismic behavior of bridge piers including soil-structure interaction. *Computers and Structures*, 43(2):373–384, 1992.

[23] J. Sweet. A technique for nonlinear soil–structure interaction. Technical Report CAI-093-100, Caltrans, Sacramento, California, 1993.

[24] Zhaohui Yang and Boris Jeremić. Numerical study of the effective stiffness for pile groups. *International Journal for Numerical and Analytical Methods in Geomechanics*, 2002. in Print, July 2003 available in preprint at: `http://sokocalo.engr.ucdavis.edu/~jeremic/publications/Piles02.pdf`.

[25] Chaiki Yoshimura, Jacobo Bielak, and Yoshaiki Hisada. Domain reduction method for three–dimensional earthquake modeling in localized regions. part II: Verification and examples. *Bulletin of the Seismological Society of America*, 93(2):825–840, 2003.

[26] Jian Zhang and Nicos Makris. Seismic response analysis of highway overcrossing including soil–structure interaction. *Earthquake Engineering and Structural Dynamics*, 31:1967–1991, 2002.